Journal of Alloys and Compounds 513 (2012) 242–244

Contents lists available at SciVerse ScienceDirect

Journal of Alloys and Compounds

journal homepage: www.elsevier.com/locate/jallcom

Influence of interfacial bonding condition on magnetoelectric properties in piezofiber/Metglas heterostructures

Yaojin Wang[a,*], David Gray[a], David Berry[b], Menghui Li[a], Junqi Gao[a], Jiefang Li[b], D. Viehland[a]

[a] Materials Science and Engineering, Virginia Tech, Blacksburg, VA 24061, USA
[b] Passive Sensors Unlimited, LLC, 2200 Kraft Drive #1200a, Blacksburg, VA 24061, USA

ARTICLE INFO

Article history:
Received 9 February 2011
Received in revised form 10 October 2011
Accepted 11 October 2011
Available online 3 November 2011

Keywords:
Magnetoelectric effect
Magnetoelectric composite
Equivalent magnetic noise
Magnetic sensitivity

ABSTRACT

The influence of the interfacial bonding condition between $Pb(Zr,Ti)O_3$ fibers and insulating Kapton films with interdigitated electrodes on the magnetoelectric (ME) response of Metglas/piezo-fiber heterostructures has been studied. An interfacial bonding method was developed, by which sensors exhibit a 1.3× enhancement in the ME coefficient (1 kHz), a 2× times reduction in the equivalent magnetic noise floor (1 Hz) and a 1.5× times increase in magnetic field sensitivity (1 Hz) relative to previous methods.

1. Introduction

Magnetoelectric (ME) coupling between magnetization and polarization in multiferroic materials has attracted much attention in recent years, not only because of undiscovered scientific underpinnings of this effect, but also due to the tremendous application potential for devices [1–3]. Single-phase ME materials are not suitable for applications due to their generally low intrinsic ME coefficients at room temperature. However, a much stronger extrinsic effect can be obtained in multi-phase composites using magnetostrictive and piezoelectric materials as active constituent phases to impart a stress-mediated product property between magnetostrictive and piezoelectric phases within the composites [3–5]. In order to enable potential applications, ME composites have been optimized in numerous aspects including the individual magnetostrictive phase [6–10], the piezoelectric phase [5,8,9], the mode of coupling, and the manner in which magnetic (H) and electric (E) fields are applied [11–13].

To date, laminated composites of magnetostrictive Metglas alloys and piezoelectric $0.7Pb(Mg_{1/3}Nb_{2/3})O_3$–$0.3PbTiO_3$ (PMN-PT) or $Pb(Zr,Ti)O_3$ (PZT) fibers possess the highest ME effects and highest sensitivity to magnetic field variations [7]. In these composites, polymer insulating films with interdigitated cooper electrodes (Kapton) were attached to both top and bottom sides of the piezofibers to form a push–pull mode configuration. The interfacial bonding condition between the Kapton and the piezo-fibers is critical to the polarization of the piezo-fibers and the ME signal detection. However, few articles have been reported on this crucial interfacial bonding. In fact, it is both physically interesting and technologically important to investigate the influence of interfacial bonding between Kapton and piezo-fibers on the ME properties of Metglas/piezo-fiber laminated heterostructures.

Here, we have fabricated three ME composites consisting of piezo-fibers, Kapton and Metglas with the same preparation process except using different methods to form the interfacial bond between Kapton and piezo-fibers. The results demonstrate a significant enhancement of the ME coefficient and magnetic field sensitivity for an optimized interfacial bonding.

2. Experimental details

Fig. 1(a) shows a schematic diagram of the ME heterostructure consisting of piezoelectric PZT fibers and magnetostrictive Metglas foils. Kapton layers with $w = 300\,\mu m$ wide interdigitated copper electrodes and $s = 1.8$ mm center-to-center spacing (Smart Materials, USA), were attached to the top and bottom sides of five PZT fibers (abreast on adhesive tape) each with dimensions of $4.2 \times 2 \times 0.2\,mm^3$ (CTS Wireless, Albuquerque, NM) using epoxy resin (Stycast 1264, USA) [7], which resulted in a lower dielectric loss. In order to prevent an asymmetry between top and bottom electrodes, the Kapton layers were attached to the PZT fibers to form a multi-push–pull mode in a two-step process. First, Kapton were laminated to the top face of the PZT fibers at 65 °C for 3 h under a vacuum pump pressure of −24 in-Hg. Second, upon removing the adhesive tape, an identical Kapton was then attached to the bottom face of the PZT fiber using the same process as above.

We developed another two steps in the bonding process, in addition to the ones given in previous reports [7]. We fabricated three different Kapton/PZT fiber composites. For composite #1, the epoxy (~100 mg) was well-distributed on the five PZT fibers, and Kapton layers were attached to the PZT fibers as described in previous

* Corresponding author. Tel.: +1 540 231 6928; fax: +1 540 231 8919.
E-mail addresses: yaojin@vt.edu, wangyaojin@hotmail.com (Y. Wang).

0925-8388/$ – see front matter © 2011 Elsevier B.V. All rights reserved.
doi:10.1016/j.jallcom.2011.10.029

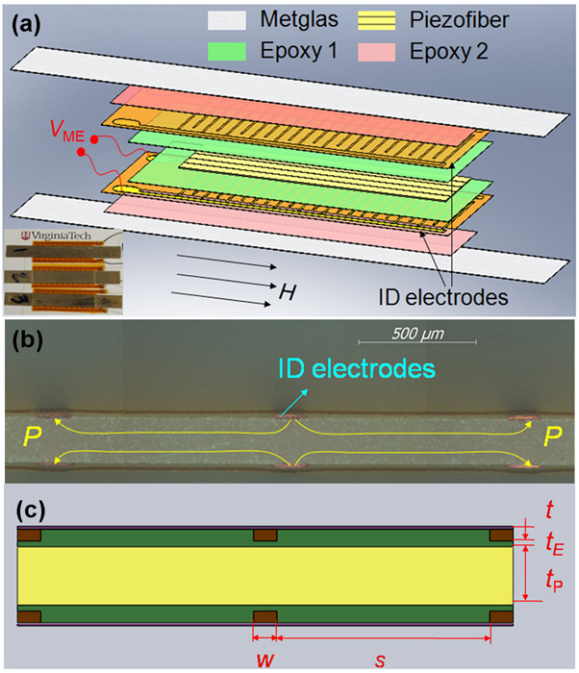

Fig. 1. (a) Schematic diagram and preparation principle of the three different PZT fiber/Metglas heterostructures. Epoxy (in red) between Metglas and Kapton is the same in the three different heterostructures, and the epoxy (in green) between Kapton and PZT fiber is the interfacial bonding, formed by different preparation process. The inset shows a photograph of the three PZT fiber/Metglas heterostructures. (b) and (c) Show an example optical microscope photograph and schematic diagram of the interfacial bonding between Kapton and PZT fibers (symmetric longitudinal poled push–pull configuration), respectively. (For interpretation of the references to color in this figure legend, the reader is referred to the web version of the article.)

reports [7]. For composite #2, the epoxy (~100 mg) was well-distributed on the Kapton layers, and the PZT fibers were attached. For composite #3, the epoxy (~50 mg) was well-distributed on Kapton layers, and then the PZT fibers were attached to the Kapton. Fig. 1(b) and (c) give a photograph and schematic diagram of the interfacial bonding between Kapton and PZT fibers, where t_E is the thickness of the Stycast epoxy layer between the ID electrodes and PZT fibers that determines the interfacial bonding region. The as-prepared composites were then polarized in silicon oil under an electric field of 15.6 kV/cm at room temperature for 15 min, where the coercive field E_C of PZT-fibers was 8.8 kV/cm.

The Metglas was commercially supplied (Vacuumscheltze GmbH & Co. KG, Germany) as a roll with a thickness of 25 μm, and was then cut to dimensions of $80 \times 10\,mm^2$. A width of 10 mm was chosen to match the total width of the five PZT fibers, and a length of 80 mm was chosen as a trade-off between maximum magnetic flux concentration and sensor size for practical applications [7]. Three such Metglas layers were then stacked one on top of each other, and bonded with epoxy resin (West System 206, USA) using a vacuum bag pressure method. These Metglas layers were then symmetrically stacked and bonded to the top and bottom sides of three different Kapton/PZT-fiber composites with epoxy resin (West System 206, USA) using a vacuum bag pressure method for more than 24 h at room temperature to form the Metglas/PZT fiber heterostructures. The induced ME voltage (V_{ME}) was directly acquired from the terminals of ID electrodes, as shown in Fig. 1(a) and (d). The photograph of the as-prepared three sensors using the previous bonding method and the modified bonding method were presented in Fig. 1(d).

Low noise operational amplifier detection circuits were then assembled following prior studies [14], and placed together in a plastic box to form detection units. A pair of NdFeB permanent magnets was affixed to the ends of the box in order to provide a dc magnetic bias H_{dc} that yielded a maximum ME voltage coefficient (α_{ME}). The ME properties of the heterostructures were characterized at zero stress bias using an in-house measurement system. The noise floor and sensitivity of the detection units, which were placed in a magnetic field shielding chambers, were measured by connecting them to a spectrum analyzer (Stanford Research, SR-785) [7].

3. Results and discussion

Fig. 2 shows α_{ME} for the three different sensors as a function of H_{dc}. It can be seen that α_{ME} for all three sensors depended

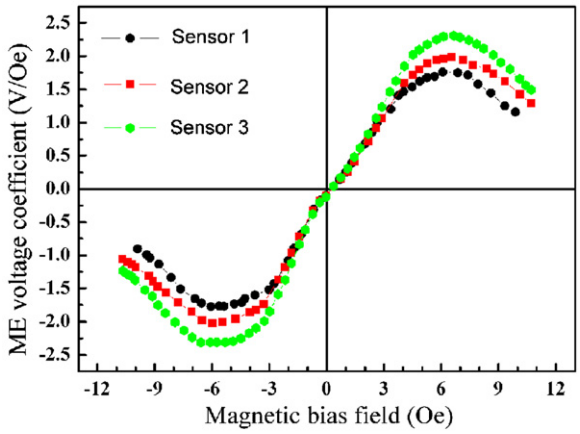

Fig. 2. ME voltage coefficient as a function of magnetic bias field for the Metglas/PZT fibers heterostructure for different preparation processes: denoted as sensor #1, sensor #2 and sensor #3, respectively.

on H_{dc} [15]. These data were taken at frequencies $f = 1$ kHz under an applied ac magnetic field $H_{ac} = 1$ Oe. We can also see that α_{ME} increases with increasing H_{dc} up to about $H_{dc} = 6$ Oe, where a maximum value is reached, above which α_{ME} subsequently decreased with increase of H_{bias}. In this figure, it can be seen that the maximum values of α_{ME} for sensors #1, #2 and #3 were 1.8 V/Oe, 2.0 V/Oe and 2.3 V/Oe. These results demonstrate that improvement of the interfacial bonding condition between Kapton and PZT fibers layers results in an increase of α_{ME} by a factor of 1.3×. Corresponding maximum values of the ME charge coefficients were 645 pC/Oe, 728 pC/Oe and 870 pC/Oe respectively. In fact, the enhancement in ME coefficient originated from the optimization of mechanical volume of core composite to magnetostrictive volume, altered by epoxy amount [7].

Next, we characterized the equivalent magnetic noise floors. Fig. 3 shows the noise floor spectrum of the three detection units over the bandwidth of $0.125\,Hz < f < 1600\,Hz$. These data were converted from the voltage noise floor ($V/\sqrt{Hz}$) directly measured from the SR-785 [14]. Using the gain of the wide band operational amplifier circuit and the ME charge coefficient of the respective sensors, in the form of a transfer function, the equivalent magnetic noise floor of the sensors was calculated, as given in Fig. 3. In this figure, the equivalent magnetic noise floor of sensor #1 was found to be lower than the other two over the entire bandwidth. The equivalent magnetic noises at 1 Hz were $4.83 \times 10^{-11}\,T/\sqrt{Hz}$, $3.74 \times 10^{-11}\,T/\sqrt{Hz}$ and $2.68 \times 10^{-11}\,T/\sqrt{Hz}$, respectively. The findings

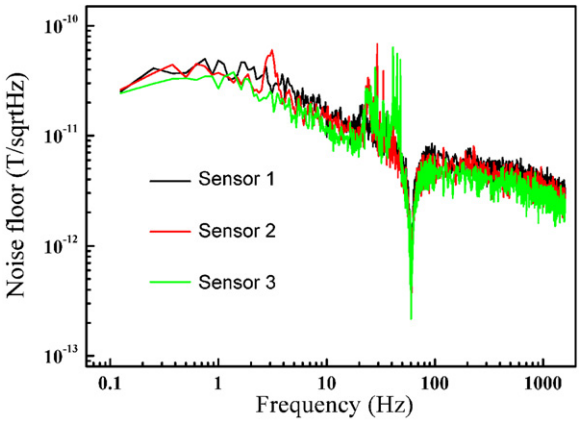

Fig. 3. Equivalent magnetic noise spectra for sensor #1, sensor #2 and sensor #3 measured in a zero-Gauss isolation chamber using a wide band charge amplifier circuit with a 60 Hz notch filter.

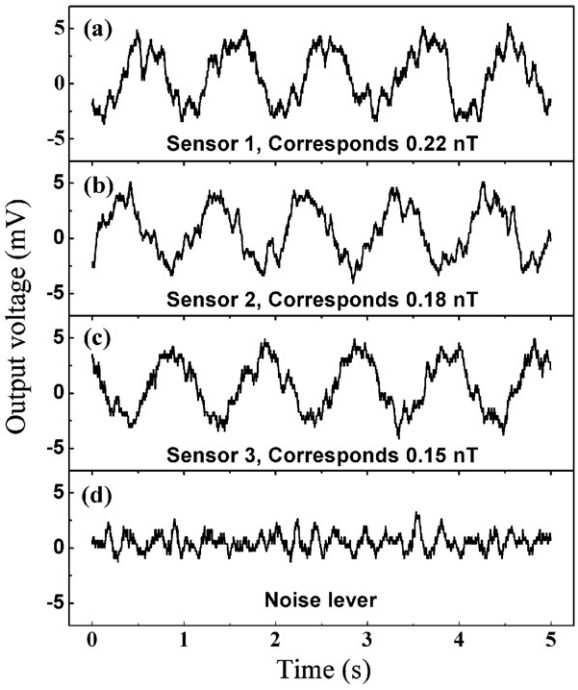

Fig. 4. Time-domain waveforms of ME output voltage at 1 Hz for (a) sensor #1, (b) sensor #2 and (c) sensor #3 using low noise charge amplifier. (e) Noise level for the detection unit as a function of real time in the absence of an incident field. The magnetic field sensitivities for a constant signal-to-noise ratio of SNR = 2 at 1 Hz is listed at the bottom of each figures.

demonstrate that an improved method of interfacial bonding can decrease the equivalent magnetic noise floor by a factor in ~2×.

Fig. 4 shows the ME voltage signal in the time domain for each sensor in response to an incident magnetic field. In the absence of an incident field, the sensor in the zero-Gauss chamber exhibited a peak-to-peak noise level of approximately 4 mV. In each plot, the magnetic field sensitivity at a constant signal-to-noise ratio of SNR = 2 at f = 1 Hz is shown. From these data, sensor #3 can be seen to detect a signal 1.5 × lower field than that of sensor #1. This is a direct consequence of the increase in the ME coefficient originating from the improved interfacial bonding.

Finally, we studied the interfacial bonding by phase angle spectra. If a fully poled state is achieved, the phase angle θ should approach 90° in the frequency range between the resonance and anti-resonance frequencies [16]. Since the three laminates were poled under identical conditions, any differences in the value of θ at resonance should reflect differences in interfacial bonding: the better interfacial bonding, the closer the value of θ should to be 90°. In Fig. 5, the phase angles can be seen to be limited to values of θ = 19°, 30° and 49° for sensors #1, #2 and #3, respectively, which were measured using Impedance Analyzer (4294 A). These results show significant differences amongst the interfacial bonding condition between the Kapton and PZT fibers for the three composites (sensors). Since sensor #3 reached closer to being fully poled than the other two, it is clear that its interfacial bonding is superior. In turn, this resulted in an enhancement of α_{ME} and a reduction in the equivalent magnetic noise floor.

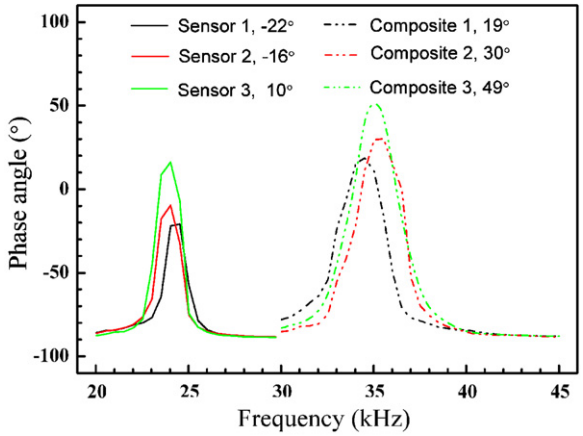

Fig. 5. Phase angle as a function of frequency for the three ME laminates and sensors near the resonance frequency region. The phase angle values at the resonance frequency are also listed in figure.

4. Conclusions

In summary, we have improved the interfacial bonding between Kapton and PZT fiber layers by a modified bonding method. The improvement has resulted an increase in the ME coefficients and a reduction in the equivalent magnetic noise floor for Metglas/PZT fiber ME heterostructures. It has been found that the optimal interfacial bonding condition resulted in a 1.3× enhancement in α_{ME} at 1 kHz, a 2× reduction in the equivalent magnetic noise floor and a 1.5× increase in the magnetic field sensitivity, compared with previous interfacial bonding methods.

Acknowledgments

This work was sponsored by the DAPPA and the Office of Naval Research.

References

[1] N.A. Spaldin, M. Fiebig, Science 309 (2005) 391.
[2] W. Eerenstein, N.D. Mathur, J.F. Scott, Nature 442 (2006) 759.
[3] Y.J. Wang, D. Gray, D. Berry, J.Q. Gao, M.H. Li, J.F. Li, D. Viehland, Adv. Mater. 23 (2011) 4111.
[4] Y. Wang, X. Zhao, J. Jiao, L. Liu, W. Di, H. Luo, S.W. Or, J. Alloys Compd. 500 (2010) 224.
[5] Y. Wang, X. Zhao, J. Jiao, Q. Zhang, W. Di, H. Luo, C.M. Leung, S.W. Or, J. Alloys Compd. 496 (2010) L4.
[6] G. Srinivasan, E.T. Rasmussen, R. Hayes, Phys. Rev. B 67 (2003) 014418.
[7] J. Das, J. Gao, Z. Xing, J.F. Li, D. Viehland, Appl. Phys. Lett. 95 (2009) 092501.
[8] L. Wang, Z. Du, C. Fan, L. Xu, H. Zhang, D. Zhao, J. Alloys Compd. 509 (2011) 508.
[9] H.-f. Zhang, S.W. Or, H.L.W. Chan, J. Alloys Compd. 509 (2011) 6311.
[10] S.Y. Chen, Y.X. Zheng, Q.Y. Ye, H.C. Xuan, Q.Q. Cao, Y. Deng, D.H. Wang, Y.W. Du, Z.G. Huang, J. Alloys Compd. 509 (2011) 8885.
[11] T. Wu, T.K. Chung, C.M. Chang, S. Keller, G. Carman, J. Appl. Phys. 106 (2009) 054114.
[12] D.T.H. Giang, N.H. Duc, Sens. Actuat. A-Phys. 149 (2009) 229.
[13] N.H. Duc, D.T.H. Giang, J. Alloys Compd. 449 (2008) 214.
[14] J. Gao, J. Das, Z. Xing, J. Li, D. Viehland, J. Appl. Phys. 108 (2010) 084509.
[15] S.X. Dong, J.Y. Zhai, J.F. Li, D. Viehland, Appl. Phys. Lett. 89 (2006) 252904.
[16] S. Wada, A. Seike, T. Tsurumi, Jpn. J. Appl. Phys. 40 (2001) 5690.